-RESEARCH PAPER-

International Journal of Mining and Geo-Engineering

IJMGE

IJMGE 56-2 (2022) 89-95

DOI: 10.22059/IJMGE.2020.298101.594844

Evaluation of scale and loading direction effects on strength and deformability of jointed rock mass: case study of Tazareh coal mine, Iran

Masoud Mazraehli [a, *], Milad Arabameri [a], Hossein Mirzaei Nasirabad [b]

[a] *Faculty of Mining, Petroleum and Geophysics Engineering, Shahrood University of Technology, Shahrood, Iran.*

[b] *Faculty of Mining Engineering, Sahand University of Technology, Tabriz, Iran.*

Article History:

Received: 17 February 2020.

Revised: 22 July 2020.

Accepted: 16 September 2020.

ABSTRACT

Determining the strength and deformation of jointed rock masses is an inevitable part of geomechanical projects. The strength and deformability of a rock mass with stochastic joint sets are conceivably anisotropic and are mainly controlled by joints' mechanical and geometrical properties. In this paper, the strength and deformation behavior of jointed rock masses against different scales and loading directions has been evaluated at the Tazareh coal mine, Iran. Field mappings through the scanline method have been used to collect joints' spatial features on rock surfaces. A statistical evaluation has been carried out on field data using Dips software. Then, the geomechanical properties of intact blocks have been measured by conducting a uniaxial compressive strength test. Finally, the rock mass is modeled using 3DEC, and its behavior is analyzed in some cases with different loading directions and block sizes to obtain representative elementary volume (REV) based on strength and deformation, respectively.

Keywords: *DEM, DFN, Experimental study, Numerical modeling, Jointed rock behavior*

1. Introduction

During the planning, construction, and utilization phases of every geomechanical project, it is essential to recognize the strength and deformability properties of jointed rock masses. Conventional techniques of strength and deformability determination can be classified into direct and indirect approaches. Direct methods include experiments on laboratory specimens and in-situ rocks. Results obtained from laboratory experiments, however, are far different from those obtained in the field because of the scale effect. On the other hand, testing intact rock samples cannot provide any information about the strength and deformation of rock masses containing fractures of different sizes and other spatial features. Hence, indirect methods are used to simulate the real behavior of jointed rocks. These techniques include empirical, analytical, and numerical models.

Empirical methods of strength and deformation estimation of rock masses stand based on the correlation between empirical data [1]. In these methods, rock mass properties are combined with a classification index which represents its geomechanical quality. Since all of the classification indices are quantitative, it is not possible to represent anisotropic and scale-dependent mechanical behavior using them.

In analytical solutions, the rock mass is defined as a mixture of intact blocks and joints (e.g. [2], [3], [4], [5], [6], and [7]), and its behavior is evaluated considering mathematical relation between loads and deformations. Fracture systems with a simplified pattern, infinite persistence, deterministic constant spacing, and specified joint orientation are involved in the derivation of this type of solution. In real conditions, however, joints have finite length, and their geometrical parameters are statistically distributed. On the other hand, the interaction between joints is not considered by this method. Therefore, real cases in which considerations of this technique are satisfied might be uncommon.

Numerical modeling is the third indirect method for evaluating the strength and deformability of rocks. In this procedure, the corresponding behavior of a rock mass is derived from a combination of strength and deformation of intact blocks and joint sets. This technique allows the contribution of different fracture networks (such as discrete fracture networks) in the rock mass properties. It also takes the interaction between joints and intact rock into account. In recent years, advanced numerical modeling tools have been utilized to involve more aspects of complex rock mass behavior during studies. For this purpose, there are two major numerical methods: (1) techniques which explicitly model discrete nature of a material (e.g. Discontinuous Deformation Analysis and Distinct Element Method); (2) Equivalent Continuum Method and its implication in Finite Difference or Finite Element Method [8].

Finite Difference and Finite Element Methods are the most widely used numerical procedures for studying the mechanical properties of geomaterials. These techniques, however, are only applicable for continuum rocks, and it is not possible to model densely fractured rock masses using them [9].

Distinct Element Method (DEM) is a robust tool for stress-strain analysis of jointed rock masses due to its advantage in the explicit demonstration of fracture network geometry and contribution of different constitutive models. Because of the complex geometry of fracture networks, numerous joint set patterns are needed for the statistical analysis of data obtained from rock mass numerical modeling [10]. Christianson et al. [11] studied strength and deformability properties of rocks through numerical simulation of triaxial, uniaxial, and tensile tests in UDEC, and stated that the trends of both numerical and experimental results are identical. Kulatilake et al. [12] numerically

* Corresponding author. *E-mail address:* mazraehli.m@shahroodut.ac.ir.com (M. Mazraehli).

investigated deformability properties of rocks with non-persistent fractures introducing fictitious joints. In the research, fictitious joints generated discrete blocks in the intersection areas with real joints. These fictitious discontinuities must imitate intact rock behavior to be distinguished from real non-persistent joints. Noorian Bidgoli et al. [13] proposed a 2D systematic numerical method to predict the strength and deformability of jointed rocks following studies conducted by Min and Jing [14] and Baghbanan [15]. They concluded that when the model size is smaller than Representative Elementary Volume (REV), the result shows a tremendous scale effect on the strength and deformation of jointed rock masses. However, when the model sizes exceed REV size, these variations would be negligible. Wu and Kulatilake [16] utilized 3DEC to determine REV, mechanical properties, and stress analysis of a rock mass that forms a dam site in china. They used crack tensor theory to combine the effects of joint sets' frequency, orientation, and size. JianPing et al. [17] used the finite element method to study the failure process, scale effect and anisotropy of uniaxial compressive strength, and deformation modulus of fractured rock masses based on a statistical constitutive model for intact rock. Their results showed that a rock mass has a critical strain which mainly is controlled by uniaxial compressive strength, rather than the deformation modulus, scale, and direction. Alshkane et al. [18] modeled a rock mass as an assemblage of deformable blocks that can yield as an intact material and/or slide along pre-existing discontinuities, and proposed a 2D numerical methodology to predict the strength and deformability of a jointed rock mass using UDEC. They concluded that the strength and deformability of rock mass significantly depend on the loading direction. Laghaei et al. [19] numerically determined compliance tensors and representative elementary volumes (REV) of a fractured rock mass with stochastic fracture systems and concluded that the characteristic parameters vary with stress path variation.

Developments in numerical modeling have resulted in providing new procedures to study the behavior of discontinuum media. The ability to define a network of non-persistent or discrete fractures is one of these developments. Understanding the strength and deformability properties of jointed rock masses and their influencing parameters is essential in different aspects of rock engineering such as the design of support systems in working stopes, selection of excavation method, slope stability, etc. Selected block size and geometrical configuration of joints with respect to loading direction are two parameters that affect the geomechanical behavior of rock mass and have not been studied yet. This paper aims to investigate the effect of geometrical properties and boundary conditions on the strength and deformability of a jointed rock mass at the Tazareh coal mine. First, data obtained from field mapping of structures are interpreted. Then, experimental intact rock testing results are provided. Finally, DEM numerical modeling is carried out to evaluate the scale and loading direction effect on rock mass behavior.

2. Tazareh coal mine

Tazareh region with a 34 km^2 area is located in the southern neighborhood of Alborz mountains, Semnan province, Iran. Coal seams in this area show a dip angle between 35 to 50 degrees, and their thicknesses vary from 0.4 to 1.8 m [20]. The geographical location of the mine has been shown in Figure 1.

Fine to coarse-graded layers of sandstone which contain quartz, with siltstone and argillite form the hanging wall of the coal seams. The footwall also generally includes siltstone and rarely sandstone and argillite [20]. The geological map and structural section of the mine are presented in Figure 2.

Mapping of discontinuities and joints is necessary to identify joint systems and study the strength-deformation behavior of rock mass. In addition, geomechanical investigation not only is important to evaluate qualitative parameters of rock mass but also to determine the spatial configuration of joints in the area. In this research, first, non-persistent joints have been mapped in the study area. Then, results including the general trend of the joints and maximum frequency related to each geometrical parameter have been calculated through statistical analysis.

Figure 1. The geographical location of the Tazareh coal mine.

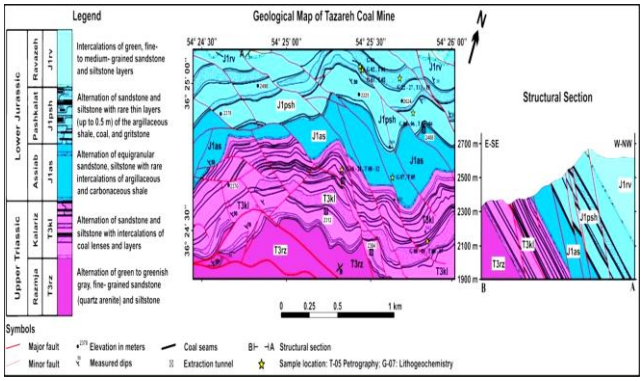

Figure 2. Geological map and longitudinal section of Tazareh coal mine [21].

The scanline method has been used for discontinuity mapping at the Tazareh coal mine. Dip and dip direction of joints have been surveyed using a compass. Other properties of fractures such as opening, persistence, surface roughness and waviness, and infill types have also been investigated. An aerial view of the mapping zone has been presented in Figure 3. According to this figure, the mapping zone is located at 36°24′24/90" northing and 54°25′21" easting next to Tunnel Madar.

Rock joints have been mapped in 3 scan lines with orientations presented in Table 1. Since the hypothetical lines with 80 degrees strike from north to east intersect most of the visible rock joints in the area, the orientations of SL2 and SL3 were selected identical to incorporate more representative structures. Persistences of the discontinuities were in the range of 0.55 to 2 meters while their dip and dip direction angles were widely different. Hence, there was a need to carry out a statistical analysis using Rocscience Dips software.

Table 1. Orientations of the scan lines.

Mapping zone location	Next to Tunnel Madar		
Scan line code	SL1	SL2	SL3
Orientation	N5E	N80E	N80E

The mechanical behavior of rock masses is extremely affected by the geometrical and mechanical properties of their weak surfaces such as joints, faults, beddings, etc. On the other hand, rock mass behavior controls the stability of a geomechanical structure. Therefore, accurate evaluation of joint systems' condition and properties is a matter of great importance for stability analysis of underground and surface excavations. Based on the analysis carried out using Rocscience Dips (Figure 4), three major joint sets have been distinguished for which average values of dip, dip direction, K fisher constants, persistence ranges, average values for roughness coefficient, aperture, and their

frequencies are listed in Table 2. It should be noted that the one-dimensional frequency or P10 was used here as a measure of jointing frequency which was calculated after clustering the mapped structures into three classes (representing the joint sets) based on the spacings recorded for each joint set.

Figure 3. Study area.

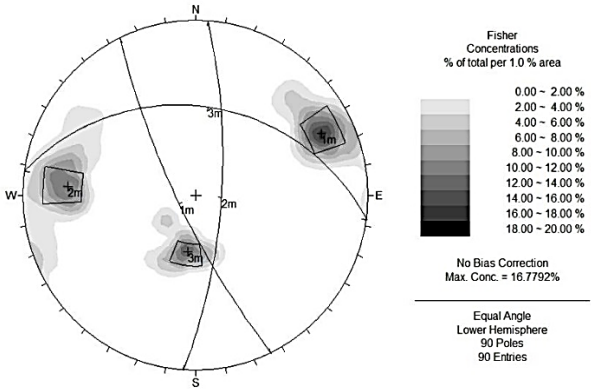

Figure 4. Stereographic demonstration of scanline data of the study area.

Table 2. Geometrical properties of distinguished joint sets in the study area.

Joint set No.	Dip angle (deg)	Dip direction (deg)	Persistence (m)	K Fisher	Roughness coefficient	Aperture (mm)	Frequency (m^{-1})
1	79.11	242.9	0.6-1.5	53.31	2.017	2.587	0.32
2	74.81	99.99	0.7-1.5	38.47	2.068	2.34	0.14
3	34.54	16.54	0.55-2	194	2.156	4.09	0.26

3. Experimental studies

Intact rock characterization is an inevitable part of every rock engineering project. In this study, uniaxial compressive tests have been carried out based on ISRM suggested method to obtain the uniaxial compressive strength (UCS) and deformability properties of the intact rock samples. Four cylindrical specimens have been taken from rock blocks that were collected from the field. When the stress-strain relationship of rock is non-linear, the modulus of elasticity (or Young's modulus) would not be a constant value. In this case, this parameter must be determined by calculating the slope of a line tangent to the axial stress-strain curve at a point of interest. In this paper, Young's modulus (and deformation modulus later on) is defined as the slope of the line connecting zero stress point to 50% of the peak strength. Results obtained from testing all of the samples are also presented in Table 3. Lateral strain values have been used to calculate Poison's ratio for the rock samples. Diameters of the specimens which have been measured before testing at their top, middle, and bottom line are also listed in Table 3.

Since sample A2 was selected next to the mapped rock face, the geomechanical characteristics of this specimen were used for simulation purposes. Figure 5 shows the sample and uniaxial compression machine before and after conducting the UCS test. Axial stress versus axial and lateral strain curves of the specimen has been illustrated in Figure 6 (a)-(b), respectively.

Table 3. Uniaxial compressive test results along with physical properties of the sample.

Sample No.	Diameter (mm)	Length (mm)	Density (g/cm^3)	Porosity (%)	UCS (MPa)	Young's modulus (GPa)	Poison's ratio
A1	54.13-54.24 54.26-54.26 54.22-54.28	135.40	2.489	0.98	130	38.00	0.24
A2	54.21-54.23 54.25-54.29 54.22-54.23	137.71	2.487	0.96	95	24.55	0.31
B1	54.26-54.29 54.29-54.31 54.29-54.32	138.40	2.878	0.67	180	49.12	0.25
B2	54.19-54.22 54.21-54.24 54.19-54.20	136.15	2.718	0.61	176	22.18	0.21

Figure 5. The specimen under uniaxial compression: a) before; and b) after testing.

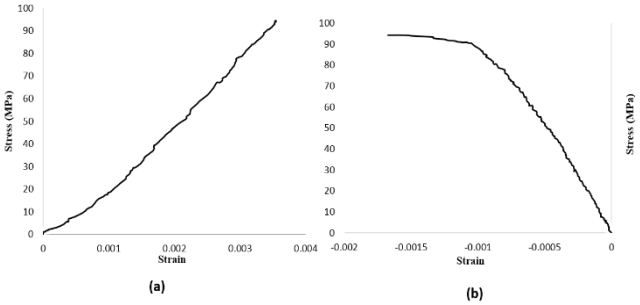

Figure 6. Axial stress vs: a) axial strain; b) lateral strain curves for the sandstone sample.

4. Numerical Modeling

The advantages of DEM in modeling jointed rock masses compared to the other numerical methods and also the importance of rock mass behavior evaluation in 3D made us utilize this method to take the mechanical effect of discrete fractures into account.

In this section, the procedure of 3D discrete fracture network (DFN) construction using geometrical parameters and their related distribution functions is introduced. ITASCA 3DEC version 5.0 software has been utilized to model Tazareh sandstone which contains discrete fractures with the obtained geomechanical properties through the

experimental study. Uniform distribution has been selected as the distribution function of fracture positions in space, and their sizes have been defined by power-law distribution considering the minimum and maximum persistence values obtained during the field mapping. In addition, fracture orientations have been generated based on Fisher distribution with the parameters presented in Table 2. In this paper, joint set 2 (out of three distinguished joint sets presented in Table 2) has not been included in the numerical model due to its lower frequency in comparison with other joint sets. Since 3DEC uses a pseudo-random logic to construct DFN, a fixed seed number has been utilized for generating the reference network of discontinuities, so that the rock blocks might be extracted from this network with no change in fractures configuration. In order to eliminate the boundary effect, researchers proposed that the interval between the block boundary and the fracture network must be larger than one-half of the largest trace length of joints located in the reference network [14]. Hence, a 3D network with 100 m sides has been selected as the reference fracture network (Figure 7).

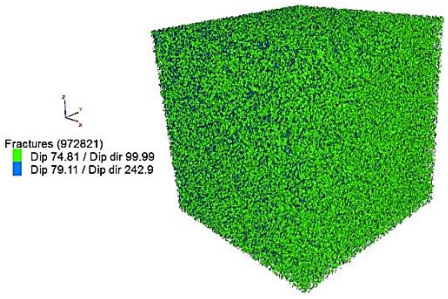

Figure 7. The reference fracture network.

The main purpose of this study is to evaluate the effect of scale and loading direction on the rock mass strength and deformability in a three-dimensional space. In order to reach this goal, it is essential to create different block sizes. These blocks, therefore, have been constructed concentrically in the reference fracture network. Consequently, twelve block models have been derived from the reference network with 0.5, 1, 1.5, 2, 2.5, 3, 3.5, 4, 5, 6, 8, and 10 m sides (Figure 8).

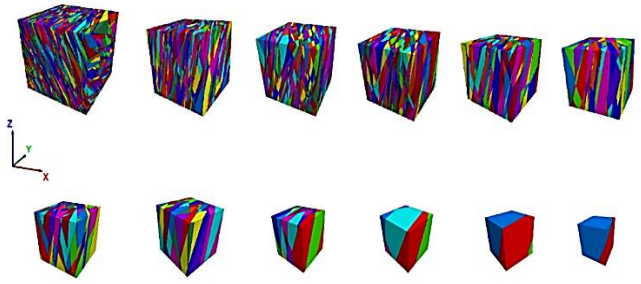

Figure 8. Jointed concentric blocks with different dimensions.

The numerical modeling process has been started with the smallest block, and the block size has been increased step by step to the block after which an increase in size doesn't significantly affect the strength behavior of the rock mass.

When under constant velocity loading, axial displacements have been recorded for all the side walls perpendicular to the loading direction. Five points shown in Figure 9 have been selected as monitoring points on the aforementioned surfaces. In the next step, a developed FISH function has been used in the software to record the average value of strain in every time step and then to calculate the total average axial and lateral strains. The stress is also calculated by averaging the stress values for all the block zones.

Geomechanical parameters used in the numerical modeling including joints normal and shear stiffness, cohesion, and internal friction angle are provided in Table 4. Furthermore, Mohr-Coulomb elastoplastic model is used to demonstrate the behavior of discontinuities. Researchers have suggested that rock mechanics' large scale effect is more due to structures than sample scale effect [22]; it is not, therefore, practical to obtain normal and shear stiffness values of a highly jointed medium in the laboratory because of the scale effect that influences the medium response. Hence, the values related to joints normal and shear stiffness are derived from Khani et al. [23].

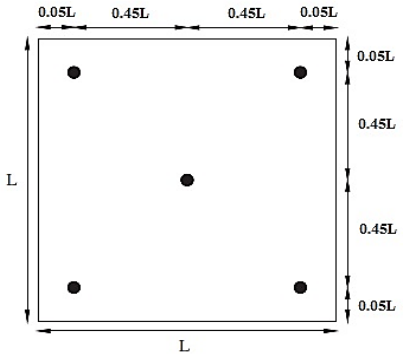

Figure 9. Location of monitoring points on each sidewall.

Table 4. Mechanical parameters of discontinuities [23].

Normal stiffness (GPa/m)	Shear stiffness (GPa/m)	Cohesion (MPa)	Internal friction angle (°)
434	434	2.5	25

4.1. Loading procedure and model calibration

Determination of appropriate loading velocity is the first step to accurately calculate the UCS and deformation modulus of rock through numerical modeling. The velocity has been determined by calibrating the numerical intact model according to the UCS test results. For this purpose, a rectangular cuboid intact block has been modeled with dimensions close to the core samples (137*54*54 mm), and a constant velocity loading has been applied to its upper surface while the lower surface has been fixed as shown in Figure 10.

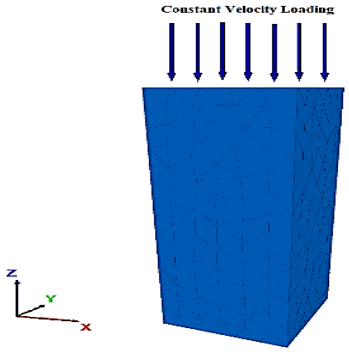

Figure 10. Intact rock numerical model under constant velocity loading.

An appropriate loading condition has been predicted solving the numerical model with different velocities and comparing the resultant stress-strain curve with the experimental one. The calibrated stress-strain curve for the intact numerical block is illustrated in Figure 11. Loading velocity for this case was 0.025 m/s. Therefore, this value has been selected as loading velocity in the forthcoming stages. The velocity, however, might cause greater strain rates compared to the real conditions but it was tried to control the velocity in a way that compressional stresses can be transferred through the entire numerical model. It could, in turn, provide the model with a continuous and constant stress rate as suggested by ISRM [24].

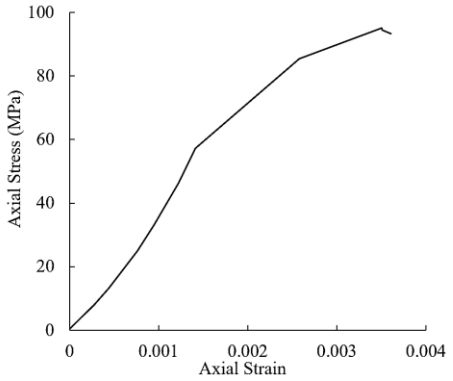

Figure 11. Axial stress vs. axial strain curve for the intact numerical model.

After the determination of appropriate velocity, it is time to define loading conditions in different directions. In order to investigate the effect of loading direction on the strength and deformation of the rock mass, blocks responses to loading in -x and -y directions are also recorded (Figure 12). In these cases, displacement of the lower sidewall perpendicular to the applied velocity is constrained like the initial loading condition.

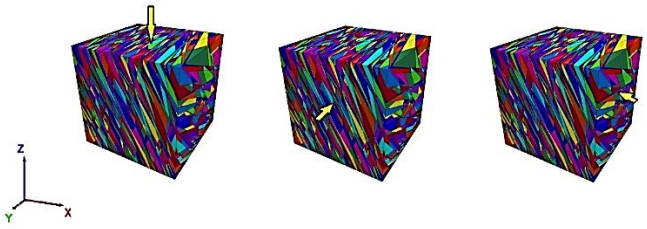

Figure 12. Loading conditions in -x, -y, and -z directions.

5. Scale effect on rock mass strength

In order to evaluate the strength behavior of block models with different sizes, constant velocity loading has been applied to the upper surface of these blocks in the z-direction. The blocks with 0.5, 2, 6, and 10 m sides have been chosen to demonstrate the scale effect. Axial stress vs. axial strain curves for these blocks are shown in Figure 13. In contrast to 0.5, 6, and 10 m side lengths, the block with 2 m long sides shows ductile post-peak behavior. This might be addressed by interactions that occurred between different joint sets in the rock mass block. Furthermore, it seems that the number of joints doesn't have a dominating role in this case compared to the other blocks' behavior.

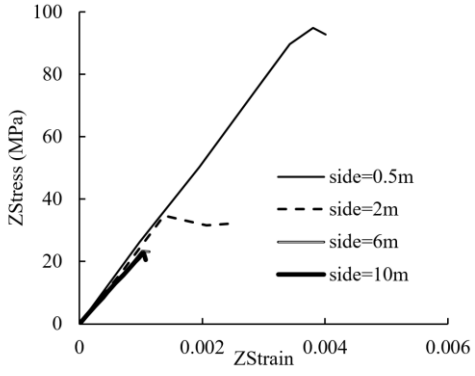

Figure 13. Axial stress-strain curves for different block sizes.

According to Figure 13, it is observed that UCS decreases significantly with increasing the block size and the number of its discontinuities. On the other hand, UCS variations for block sizes in the range of 6 to 10 m are negligible. It should be noted that there are some fluctuations in the numerically obtained curves which may be addressed with the instability that occurred for blocks during the loading process. For comparison purposes, these curves have been refined to eliminate the fluctuations as shown in Figure 13. The original curves are presented in Figure 14 in which some irregularities can be observed.

6. Determination of Representative Elementary Volume based on the strength

In numerical modeling, there is a minimum block size after which increasing the block size doesn't significantly affect a given model feature [16]. This block size which is statistically homogenous and contains a certain number of discontinuities may be referred to as REV and can be used to represent its equivalent rock mass. Strength-based REV is calculated using the procedure illustrated in Figure 15 which depicts UCS against the block size. It is observed that the UCS variation is negligible for block sizes more than 3 m. Therefore, a block with 3 m sides is introduced as REV based on strong values.

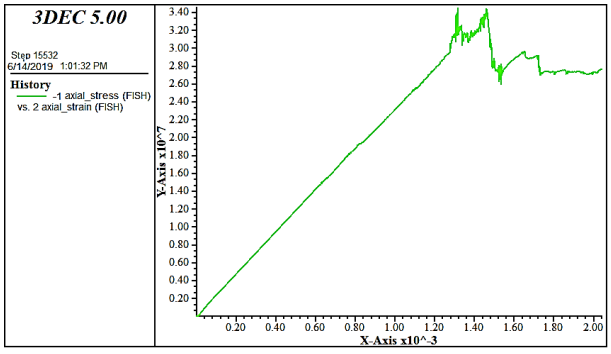

(a)

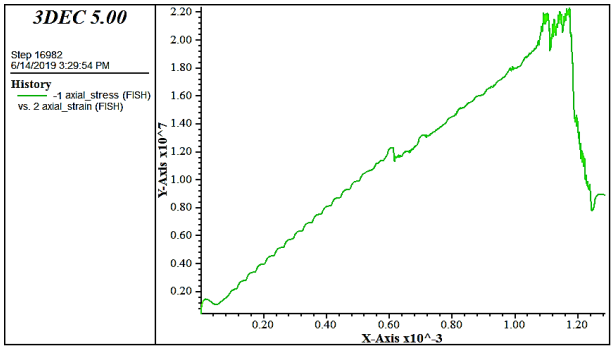

(b)

Figure 14. Original stress vs strain curves for a) 2 m, and b) 6 m side lengths.

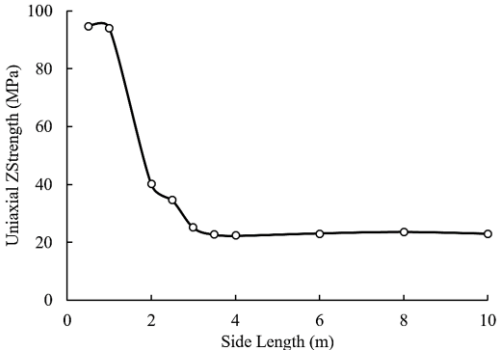

Figure 15. REV determination based on strength.

7. Loading direction effect on rock mass strength

Jointed rock mass behavior is always affected by loading direction because of geomechanical properties anisotropy. In this section, the mechanical behavior of Tazareh jointed sandstone is studied under axial loads in –x and –y directions.

Figure 16 shows the axial stress vs axial strain curves for selected blocks with 0.5, 2, 6, and 10 m sides. Comparison of these curves with each other and with the stress-strain curve of the simulated intact rock helps us discover the jointing, scale, and loading direction effect on strength of the jointed blocks when loading in different directions.

It should be noted that Figure 16 (a) and (b) demonstrates the results obtained from simulated rock mass with different side lengths loaded in x and y directions, respectively, while Figure 11 presents a simulated intact rock loaded in the z-direction. In the latter case, the rectangular cubic sample size was considered large enough to be equivalent to its cylindrical lab sample. For the former case, however, the side lengths were increased from 0.5 to 10 m for square blocks, and the determination of REV size is the main goal of the simulated tests. It is, therefore, expected that a sample with 0.5 m side length has an uniaxial strength close to the intact sample since the averaged spacings of considered joint sets (according to Table 2) are in a range between 3.125 and 3.846 m.

It is also remarkable that the strength value for the lowest block size when loading in –y direction is more than the other cases. Comparison between Figure 16 (a) and (b) with Figure 13 shows that the scale effect is more obvious when loading in –x direction. According to Figure 16 (a), increasing the block size makes the slope of the stress-strain curve vary more than the other cases.

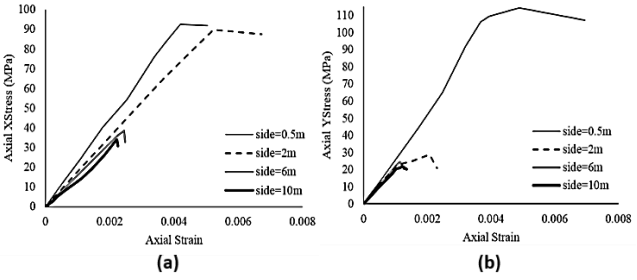

Figure 16. Axial stress vs axial strain curves when loading in: a) –x; and b) –y direction.

8. Loading direction effect on strength-based REV

In this section, the effect of loading direction on REV determination based on the UCS of the blocks is evaluated. Figure 17 illustrates numerical results obtained for different block sizes when loading in –x, -y, and –z direction, respectively.

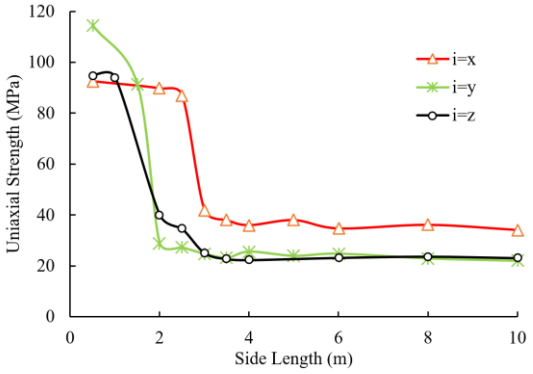

Figure 17. Loading direction effect on strength-based REV.

Loading direction effect on jointed rock mass strength is clear in Figure 15 for different block sizes. It is also observed in the diagram that strength-based REV is different for these three cases. It is, therefore, concluded that the loading direction influences REV determination. According to Figure 17, REV is equal to 3 m for –x and –z loading cases, and 2.5 m for –y loading cases.

In the next step, trends of stress-strain curves are compared for the given block size. In order to carry out a correct comparison, this block size must be equal to or more than REV for all the loading conditions. Thus, the block with 3 m long sides is applicable for this purpose because it is equal to or is bigger than REVs for three cases. Axial stress versus axial strain curves applying different loading conditions is shown in Figure 18. It is obvious that the peak strength when loading in –x direction is more than the other ones. On the other hand, the deformation modulus for this case is the lowest.

9. Loading direction effect on deformability-based REV

The slope of the axial stress-strain curve represents rock mass deformation modulus. As stated before, block size and loading direction both affect deformation modulus. In this section, scale and loading direction effect on the determination of deformation-based REV is investigated. The same procedure as the last section is used to determine REV based on deformation modulus. For this purpose, the numerical results obtained for deformation modulus are depicted in Figure 19 against block sizes when loading in different directions. Deformation modulus has been calculated using the 50% peak strength of each block and its corresponding strain. Figure 19 shows that the deformation modulus is higher when loading in –y and –z directions, and it is reduced up to a certain block size which equals 2 m when loading in –x and –y directions, and 4 m when loading in –z direction.

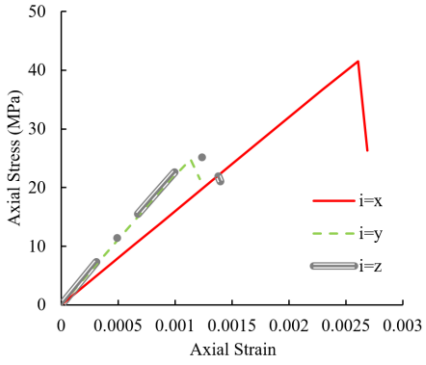

Figure 18. Axial stress vs axial strain curves for 3 m block size.

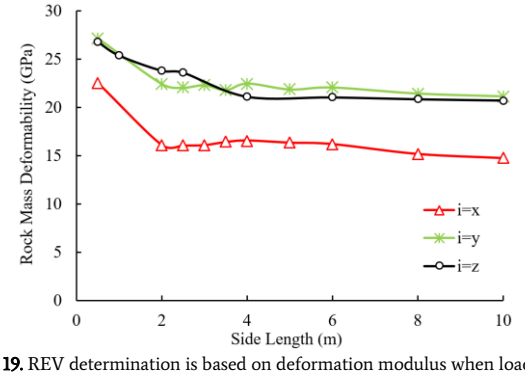

Figure 19. REV determination is based on deformation modulus when loading in different directions.

10. Conclusions

The study of strength and deformation behavior of coal-bearing formations is important in many aspects such as evaluating hanging wall competency of coal seams, designing underground openings, etc. Experimental tests on intact rock samples, however, cannot provide useful information about rock mass behavior. Despite in-situ large-scale tests being the most reliable methods for predicting rock mass strength

and deformation, these methods suffer from economical and time-related problems. Therefore, it is reasonable to use numerical methods as an alternative for the aforementioned tests. Tazareh coal mine is one of the most important mines in Iran. In terms of lithology, the area consists of sandstone, siltstone, argillite, and coal seams intercalations. Sandstone frequently comprises hanging walls of the coal seams. In this paper, scale and loading direction effect on strength and deformability of Tazareh sandstone was investigated collaborating field mapping of structures, experimental intact rock testing, and DEM numerical modeling. The results show that numerical model size affects values obtained for strength and deformation modulus so that increasing the block size decreases strength value up to a REV size after which the variation is negligible. A block with 3 m long sides was determined as REV based on strength value, and its strength was equal to 25 MPa. A block with 2 m long sides was estimated as deformation-based REV size when loading in –x and –y directions. Appling constant velocity in –z direction, the corresponding block size was 4 m. Deformation modulus for REV was 16, 22.4, and 21.1 when loading in –x, -y, and –z directions, respectively.

REFERENCES

[1] Hoek, E. & Brown, E. T. (1997). Practical estimates of rock mass strength. International Journal of Rock Mechanics and Mining Sciences. 34(8), 1165-1186.

[2] Salamon, M. D. G. (1968). Elastic Moduli of a Stratified Rock Mass. International Journal of Rock Mechanics and Mining Sciences. 5,519-527.

[3] Singh, B. (1973). Continuum Characterization of Jointed Rock Masses. International Journal of Rock Mechanics and Mining Science and Geomechanics Abstract. 10,311-335.

[4] Morland, L. (1976). Elastic anisotropy of regularly jointed media. Rock Mechanics. 8,35-48.

[5] Amadei, B. & Goodman, R. E. (1981). A 3-D Constitutive Relation for Fractured Rock Masses. Proceedings of International Symposium on the Mechanical Behavior of Structured Media, Ottawa, pp. 249-268.

[6] Gerrard, C. M. (1982). Equivalent Elastic Moduli of a Rock Mass Consisting of Orthorhombic Layers. International Journal of Rock Mechanics and Mining Science and Geomechanics Abstract, 19, 9-14.

[7] Fossum, A. F. (1985). Effective Elastic Properties for a Randomly Jointed Rock Mass. International Journal of Rock Mechanics and Mining Sciences, 22(6), 467-470.

[8] Zhang, L. (2010). Method for Estimating the Deformability of Heavily Jointed Rock Masses. Journal of Geotechnical and Geoenvironmental Engineering, 136(9), 1242-1250.

[9] Yang, J. P., Chen, W. Z., Dai, Y. H., & Yu, H. D. (2014). Numerical determination of elastic compliance tensor of fractured rock masses by finite element modeling. International Journal of Rock Mechanics and Mining Sciences, 70, 474-482.

[10] Priest, S. D. (1993). Discontinuity analysis for rock engineering. Springer.

[11] Christianson, M.C., & Board, M. P. (2006). UDEC Simulation of triaxial testing of lithophysal tuff. Proceedings of the 41st U.S. Symposium on Rock Mechanics (USRMS) and 50th Anniversary of the U.S. Rock Mechanics Association, pp. 968.

[12] Kulatilake, P., Wang, S., & Stephansson, O. (1993). Effect of finite size joints on the deformability of jointed rock on three dimensions. International Journal of Rock Mechanics and Mining Sciences & Geomechanics Abstracts. 30(5), 479-501.

[13] Noorian Bidgoli, M., Zhao, Z., & Jing, L. (2013). Numerical evaluation of strength and deformability of fractured rocks. Journal of Rock Mechanics and Geotechnical Engineering, 5, 419-430.

[14] Min, K. B., & Jing, L. (2003). Numerical determination of the equivalent elastic compliance tensor for fractured rock masses using the distinct element method. International Journal of Rock Mechanics & Mining Sciences. 40, 795-816.

[15] Baghbanan, A. (2008). Scale and stress effects on hydro-mechanical properties of fractured rock masses. Ph.D. Thesis, KTH Royal University.

[16] Wu, Q., & Kulatilake, P. (2012). REV and its properties on fracture system and mechanical properties, and an orthotropic constitutive model for a jointed rock mass in a dam site in China. Computers and Geotechnics, 43, 124-142.

[17] JianPing, Y., WeiZhong, C., DianSen, Y., & JingQiang, Y. (2015). Numerical determination of strength and deformability of fractured rock mass by FEM modeling. Computers and Geotechnics, 64, 20-31.

[18] Alshkane, Y. M., Marshall, A. M., & Stace, L. R. (2017). Prediction of strength and deformability of an onterlocked blocky rock mass using UDEC. Journal of Rock Mechanics & Geotechnical Engineering, 9, 531-542.

[19] Laghaei, M., Baghbanan, A., Hashemolhosseini, H., & Dehghanipoodeh, M. (2018). Numerical determination of deformability and strength of 3D fractured rock mass. International Journal of Rock Mechanics & Mining Sciences, 110, 246-256.

[20] Supervising office (2009). Apprenticing report of Tazareh coal mine. Eastern Alborz Coal Company, Shahrood, Iran.

[21] Tatar, A., Alipour Asll, M. (2019). Geochemistry of major, trace, and rare earth elements in coals from the Tazareh mine, Eastern Alborz Coalfield, NE Iran. Geochemistry: Exploration, Environment, Analysis.

[22] Alejano, L. R., Arzua, J., Bozorgzadeh, N., & Harrison, J. P. (2017). Triaxial strength and deformability of intact and increasingly jointed granite samples. International Journal of Rock Mechanics & Mining Sciences, 95, 87-103.

[23] Khani, A., Baghbanan, A., & Hashemolhosseini, H. (2013). Numerical investigation of the effect of fracture intensity on deformability and REV of fractured rock masses. International Journal of Rock Mechanics and Mining Sciences, 63, 104-112.

[24] International Society for Rock Mechanics., Commission on Standardization of Laboratory and Field Tests. Committee on Laboratory Tests (1978). Suggested methods for determining the uniaxial compressive strength and deformability of rock materials.